Supplemental Material

Supplemental Methods:

Animal carcinogenesis studies

All mice were housed in a pathogen-free animal facility at Washington University in accordance with animal care regulations. In order to test the tumor-promoting potential of chronic ACD, we modified the standard contact hypersensitivity protocol (Figure 1D)(7). 4-8-week old female mice were shaved on their abdomen and back. They were sensitized to 50μl of 1% DNFB in acetone applied to their abdominal skin on day 0. A week later, the back skin of each animal was treated with 100μg DMBA in 200μl acetone. One week later, mice were randomized to three groups; two groups received 3cm surgical incision followed by 6.0 silk suture placement and 100μl of 0.5% DNFB or acetone treatments on their back. The third group received DNFB without surgical wound. In experiments involving Rag-deficient animals (Figure 2E and 2F), all the animals received 3cm surgical incision. Animals continued to receive allergen versus carrier treatment every 2-3 days at doses that maintained a mild chronic dermatitis in the wild-type test cohort. Note that olive oil was added to acetone at the ratio of 1:4 (olive oil : acetone) to reduce the degree of skin irritation from the chemical treatments. Animals' nails were clipped at regular intervals to minimize any skin excoriations. Mice were photographed with a digital camera regularly and monitored for onset, number and size of tumors and any sign of failure to thrive. Moribund mice were euthanized and their tissues were harvested.

Histology, Immunofluorescence, and Immunohistochemistry

Patient Samples: Formalin-fixed paraffin-embedded tissue sections (4mm) were immunostained

using a Ventana Ultra automated immunostainer (Ventana Medical Systems, Tucson, AZ). Following deparaffinization, antigen retrieval was performed at 95°C for 65 min using Ultra Cell Conditioning Solution (ULTRACC1). For double-staining immunohistochemistry for CD3/T-bet and CD3/GATA-3, slides were sequentially reacted first with an anti-CD3 antibody (clone PS1, Biocare Medical, Concord, CA), followed by incubation with ultraView Universal Alkaline Phosphatase Red Detection Kit (Ventana Medical Systems), and then with either anti-T-bet (clone MRQ-46, Cell Marque, Rocklin, CA) or anti-GATA-3 (clone L50-823, Biocare Medical) antibodies, which were followed by incubation with ultraView Universal DAB Detection Kit (Ventana Medical Systems) and hematoxylin counterstaining. For single stains, anti-Tryptase (clone G3, Ventana Medical Systems), anti-CD31 (clone JC70, Ventana Medical Systems), anti-CD68 (clone KP-1, Ventana Medical Systems), anti-CD163 (MRQ-26, Ventana Medical Systems) and anti-E-cadherin (EP700Y, Ventana Medical Systems) were used.

Animal Studies: Dorsal skin and tumor samples were harvested from mice and fixed in 2% paraformaldehyde-lysine-phosphate at $4^{\circ C}$ for 6 hours followed by 30% sucrose solution overnight. Portion of samples were embedded in OCT Freezing medium (Sakura Finetek, Torrance, CA) and rapidly frozen. Frozen sections were cut at 9μm, mounted on glass slides, and incubated with combinations of anti-mouse CD3 (BD Biosciences, Franklin Lakes, NJ), CD4 (BD Biosciences), CD31 (BD Biosciences), F4/80 (eBioscience, Inc., San Diego, CA), CD206 (BioLegend, San Diego, CA) & biotin-conjugated anti-Cytokeratin 14 (K14; Thermo Fisher Scientific Inc., Waltham, MA) followed with APC-conjugated streptavidin. DAPI nuclear stain (Vector Labs, Burlingame, CA) was used to counterstain sections. Remaining portions of sections were prepared for Hematoxylin and eosin (H&E) and toluidine blue staining using paraffin-embedded tissue sections of skin and tumor samples. These tissues were fixed in 2% paraformaldehyde-lysine-phosphate, dehydrated with ethanol and embedded in paraffin, which were then sectioned at 5μm. Histology images were taken using fluorescent microscope or

NanoZoomer (Hamamatsu Photonics K.K., Japan).

Quantitative RT-PCR

Dorsal skin and tumor samples were homogenized in RLT Lysis Solution using a Mini-BeadBeater-8 (BioSpec Products, Inc., Bartlesville, OK). Total RNA from homogenized tissue was isolated using an RNeasy Mini Kit (Qiagen, Netherlands, Venlo, Limburg) and quantity was determined using a NanoDrop ND-1100 (NanoDrop Technologies). cDNA was synthesized using 1μg of total RNA with Invitrogen SuperScript II Reverse Transcriptase (Life Technologies, Carlsbad, CA). Transcript levels of cDNA were measured utilizing a 7300 Real-Time PCR System (Applied Biosystems, Foster City, CA) with iTaq™ Universal SYBR® Green Supermix (Bio-Rad Laboratories, Hercules, CA) or TaqMan Universal Master Mix II 4440040 (Applied Biosystems). The following primer sets were used for SYBR green analysis (all primers are shown 5' to 3'): *IL-6* Fwd - AGGCGCCCAACTGTGCTAT, *IL6* Rev - TCTCCTGCGTGGAGAAAAGG, *IFN-γ* Fwd - GATATCTGGAGGAACTGGCAAAAG, *IFN-γ* Rev - AGAGATAATCTGGCTCTGCAGGAT, and *gapdh* Fwd - AATGTGTCCGTCGTGGATCTGA, *gapdh* Rev - GATGCCTGCTTCACCACCTTCT. PrimeTime Assays (Integrated DNA Technologies, Coralville, Iowa) were used for TaqMan analysis: *IL-4* - Mm.PT.28.32703659, *IL-17a* - Mm.PT.58.6531092, *IL-23a* - Mm.PT.581059418.g, *gapdh* - Mm.PT.39a.1. Transcript levels were normalized to *gapdh* levels.

Supplemental Figures

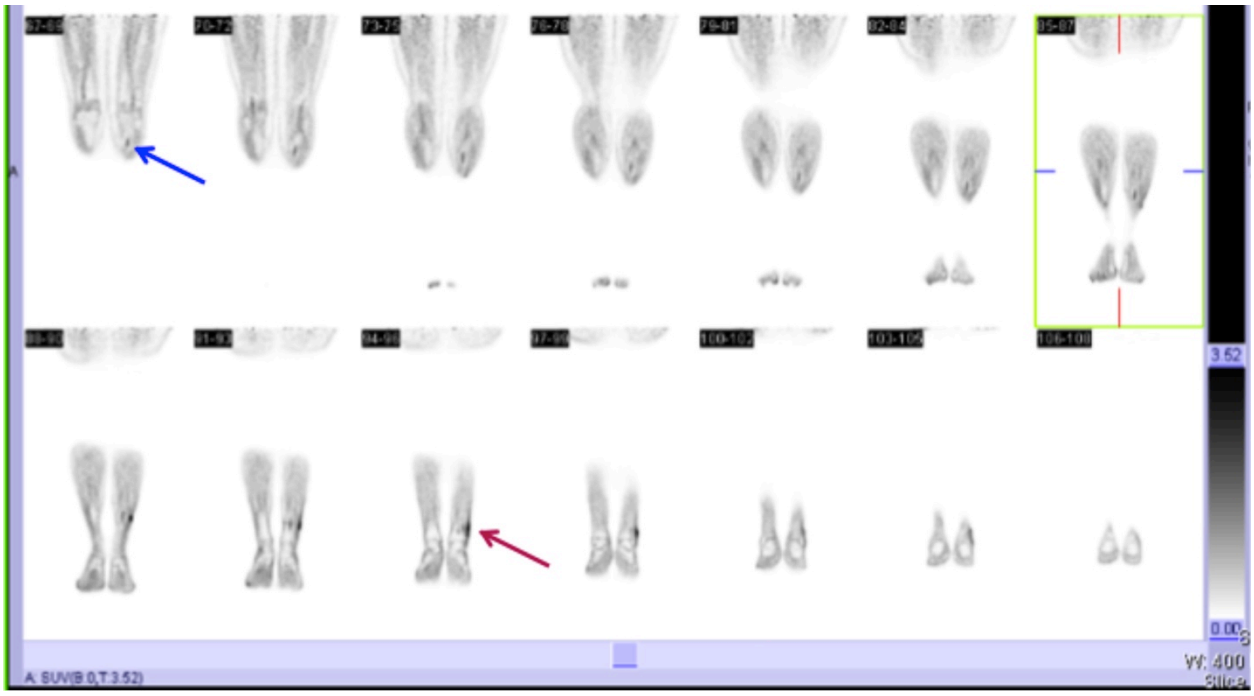

Supplemental Figure 1. Positron emission tomography–computed tomography (PET-CT) scan of patient's legs highlights the fluorodeoxyglucose (FDG) uptake at the site of SCC on left lateral ankle (red arrow) and a lymph node in popliteal fossa (blue arrow). Subsequently this lymph node was biopsied and found to be reactive with no evidence of cancer metastasis.

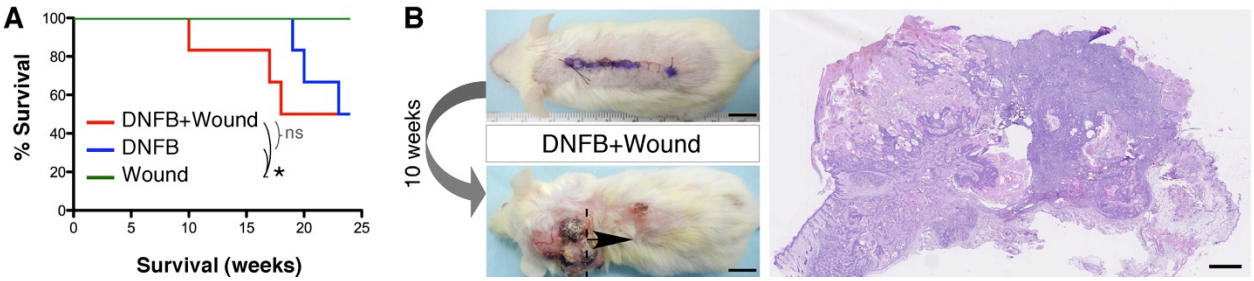

Supplemental Figure 2. Chronic allergic contact dermatitis (ACD) results in development of invasive squamous cell carcinoma (SCC) in mice (related to Figure 1). (**A**) High rate of tumor progression from papillomas to SCCs led to demise of a subgroup of animals treated with DNFB (*: $p < 0.05$, log rank test). (**B**) Representative image shown of mouse treated with DNFB and receiving a surgical wound (scale bar: 1cm) which led to development of an aggressive SCC (scale bar: 1mm). Note the short latency (i.e. ten weeks) to develop a large SCC in response to DNFB. Age-matched FVB female mice were used in this study; n = 6 per group; ns: not significant.

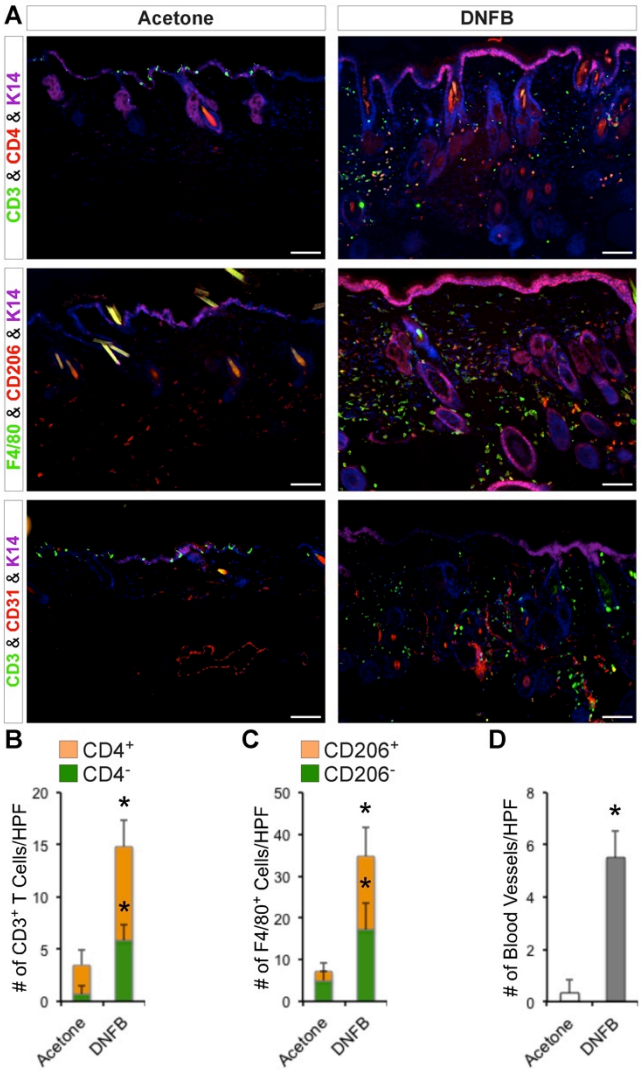

Supplemental Figure 3. The number of tumor-promoting dermal cells is significantly increased in the DNFB-treated mice compared to the acetone-treated controls (related to Figure 2A). (**A**) $CD4^+$ T cells, $F4/80^+$ $CD206^+$ alternatively activated (M2) macrophages, and $CD31^+$ endothelial cells (marking the blood vessels) in the dermis of the DNFB- and acetone-treated mice are compared. Representative images are shown (scale bar: 100μm). The average number of dermal (**B**) $CD3^+$ $CD4^+$ and $CD3^+$ $CD4^-$ T cells, (**C**) $F4/80^+$ $CD206^+$ (M2) and $F4/80^+$ $CD206^-$ macrophages, and (**D**) blood vessel cross-sections in 6 random high power microscopic fields (HPFs) of the skin treated chronically with DNFB is compared to acetone-treated controls (*: $p < 0.01$, Student's *t*-test).

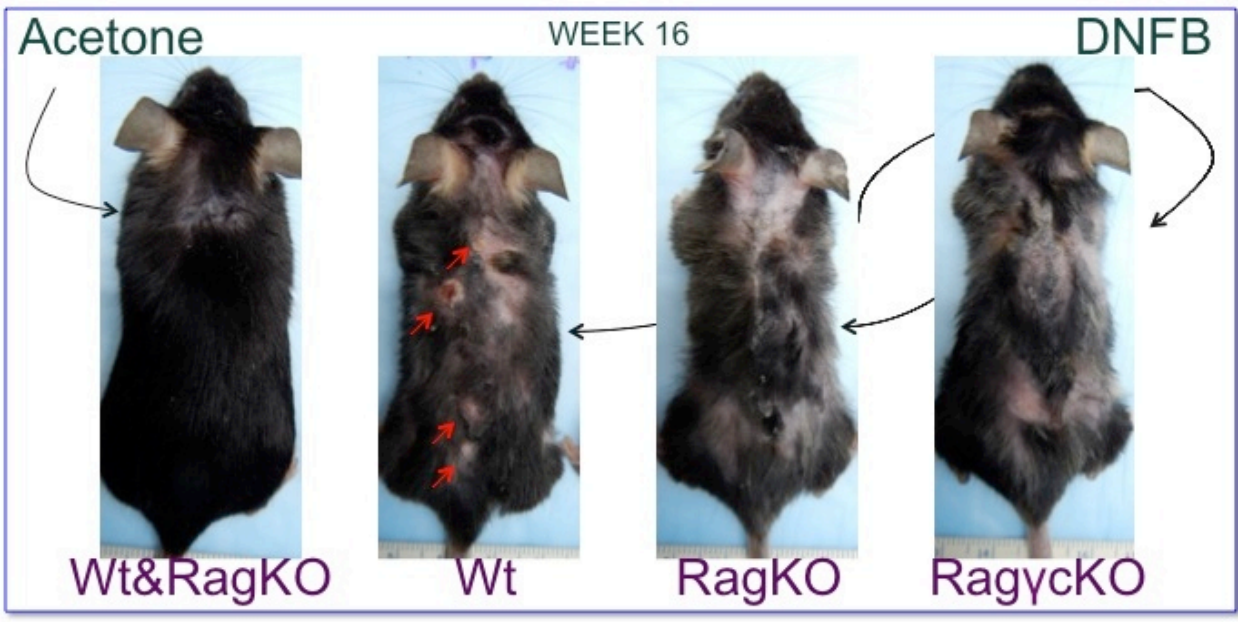

Supplemental Figure 4. The representative pictures of wild-type mice treated with acetone versus wild-type, *Rag1*$^{-/-}$ (RagKO) and *Rag2*$^{-/-}$*, γc*$^{-/-}$ (RagγcKO) treated with DNFB show the similar degree of hair loss and skin irritation in all the animals treated with DNFB (related to Figure 2E and 2F). Red arrows point to the skin tumors in wild-type mouse treated with the allergen.

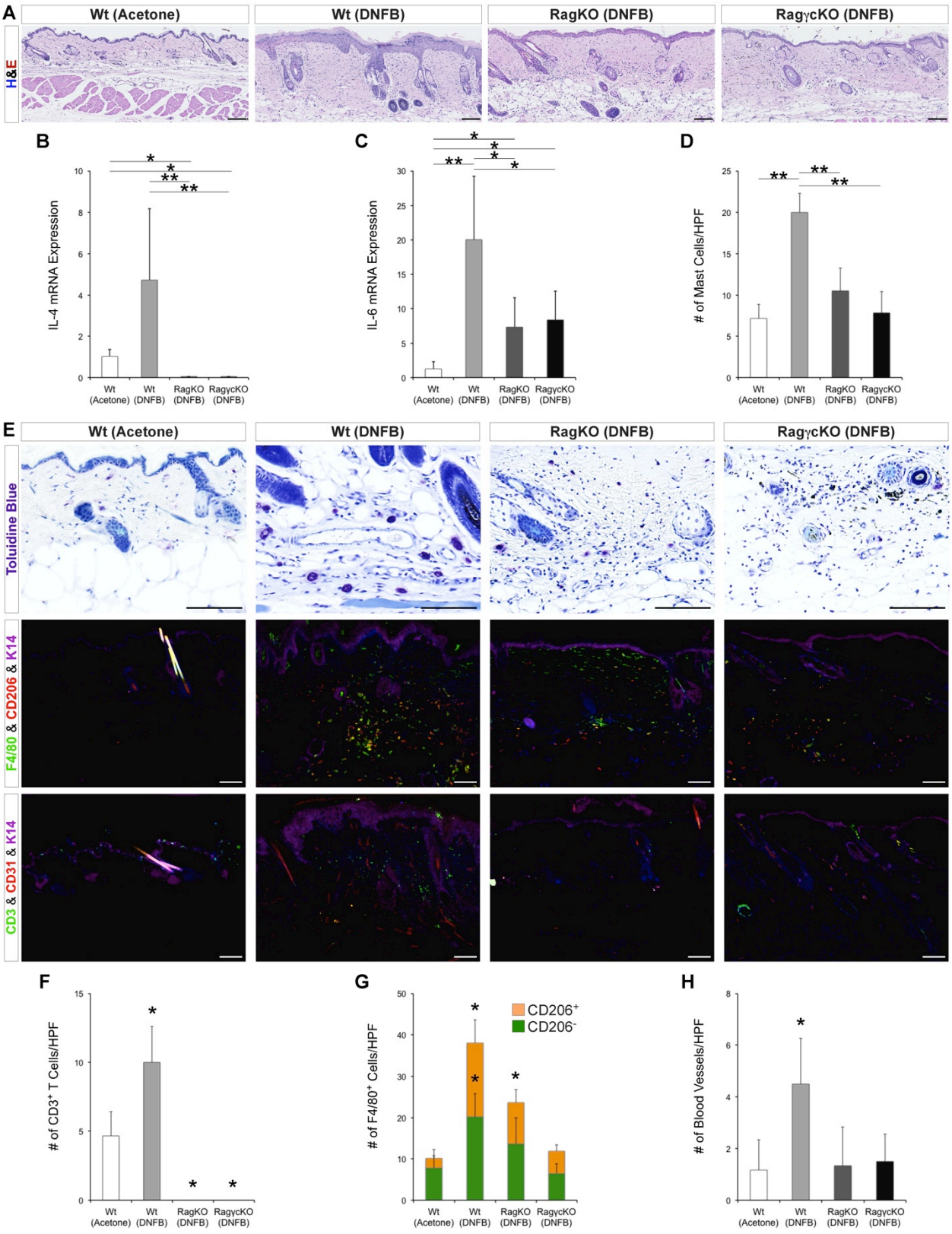
A
Wt (Acetone)
Wt (DNFB)
RagKO (DNFB)
RagγcKO (DNFB)
H&E
B
IL-4 mRNA Expression
C
IL-6 mRNA Expression
D
# of Mast Cells/HPF
Wt (Acetone)
Wt (DNFB)
RagKO (DNFB)
RagγcKO (DNFB)
E
Toluidine Blue
F4/80 & CD206 & K14
CD3 & CD31 & K14
F
# of CD3+ T Cells/HPF
G
# of F4/80+ Cells/HPF
CD206+
CD206-
H
# of Blood Vessels/HPF

Supplemental Figure 5. Tumor-promoting factors associated with DNFB-driven inflammation are suppressed in DNFB-treated *Rag1*$^{-/-}$ (RagKO) and *Rag2*$^{-/-}$*, γc*$^{-/-}$ (RagγcKO) mice. (**A**) Representative images of H&E-stained skin from the animals treated with DNFB x14 weeks and their acetone-treated controls are shown (related to Figure 2E and 2F). Note the extent of epidermal hyperplasia and dermal inflammation in the DNFB-treated wild-type animals that is significantly diminished in RagKO and RagγcKO mice. (**B** and **C**) qRT-PCR analysis of (**B**) IL-4 and (**C**) IL-6 expression in the skin of mice treated with DNFB versus acetone is shown (n = 4 in each group; *: $p < 0.05$, **: $p < 0.01$, Student's *t*-test). (**D**) The average number of mast cells in 6 random high power microscopic fields (HPFs) of the skin of wild-type, RagKO and RagγcKO mice treated chronically with DNFB is compared to acetone-treated mice (*: $p < 0.05$, **: $p < 0.01$, Student's *t*-test). (**E**) Representative pictures of skin sections stained with toluidine blue for mast cells, F4/80 and CD206 for M2 macrophages (F4/80$^+$ CD206$^+$) and CD31 for blood vessels in the dermis of the DNFB- and acetone-treated mice are shown. Note the smaller size of mast cells and reduced number of M2 macrophages and blood vessel density in DNFB-treated in RagKO and RagγcKO skin (scale bar: 100μm). The average number of dermal (**F**) CD3$^+$ T cells, (**G**) F4/80$^+$ CD206$^+$ (M2) and F4/80$^+$ CD206$^-$ macrophages, and (**H**) blood vessel cross-sections in 6 random HPFs of the skin are shown (*: $p < 0.01$, compared to acetone-treated wild-type animals, Student's *t*-test).

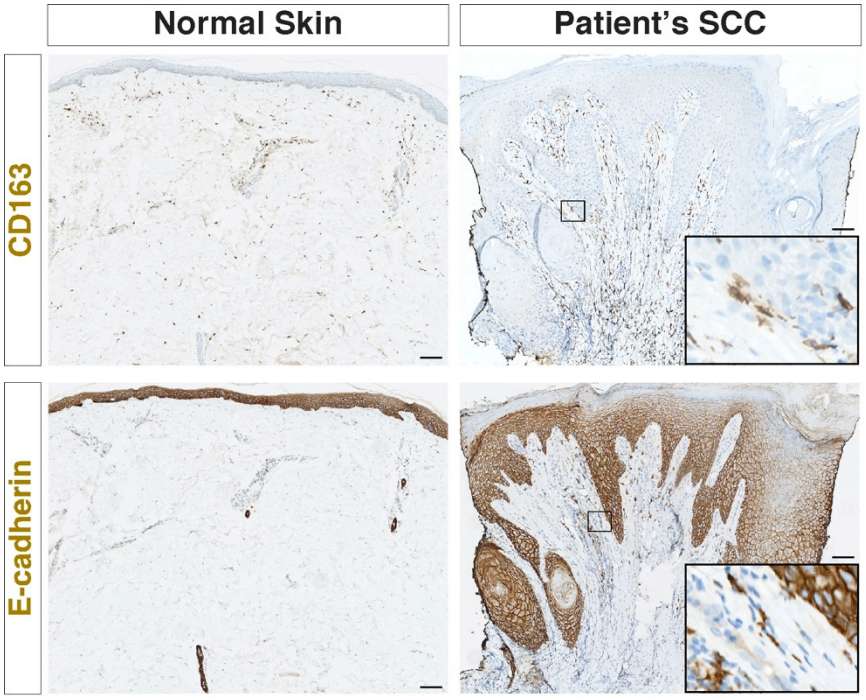

Supplemental Figure 6. Alternatively activated (M2) macrophages are associated with patient's SCC. CD163 and E-cadherin staining on adjacent sections highlight the accumulation of $CD163^{+}$ $E\text{-}cadherin^{+}$ M2 macrophages in patient's skin at the site of SCC (punch biopsy). Note the morphology of $CD163^{+}$ $E\text{-}cadherin^{+}$ cells in the dermis (insets). Scale bar: 100μm.

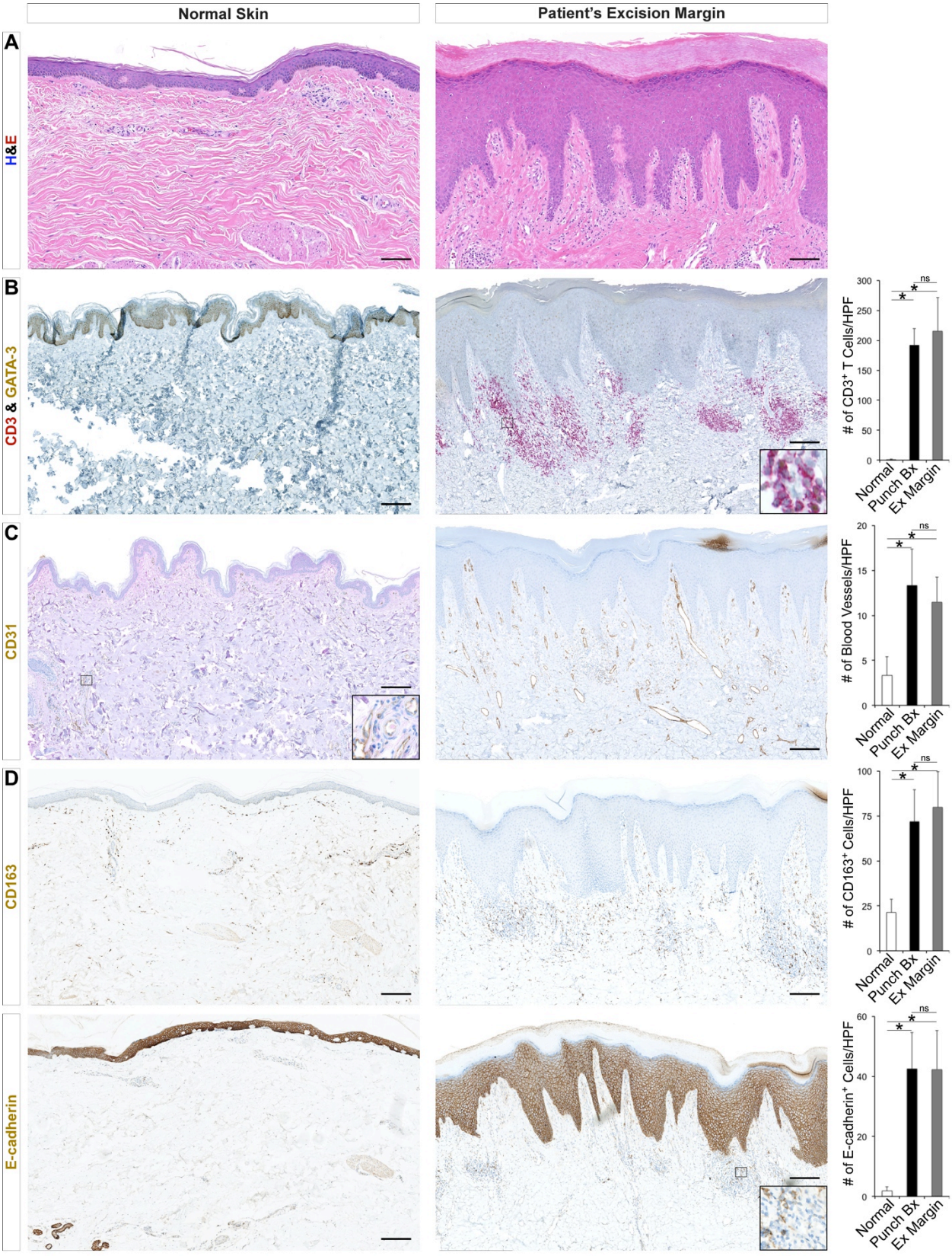
Normal Skin
Patient's Excision Margin
A
H&E
B
CD3 & GATA-3
# of CD3+ T Cells/HPF
C
CD31
# of Blood Vessels/HPF
D
CD163
# of CD163+ Cells/HPF
E-cadherin
# of E-cadherin+ Cells/HPF
Normal
Punch Bx
Ex Margin
ns
*

Supplemental Figure 7. Tumor-promoting inflammation extends to the cancer-free margins of the skin excised from the patient's left lateral ankle. (**A**) H&E staining, (**B**) CD3 plus GATA-3 staining for Th2 cells, (**C**) CD31 staining for blood vessels, and (**D**) CD163 and E-cadherin stainings on adjacent sections for M2 macrophages are shown. Note that the morphology of E-cadherin^{+} cells in the dermis of the patient's skin is consistent with marking cells of macrophage lineage (inset). The average number of dermal cells and blood vessels in normal skin, patient's punch biopsy (Punch Bx) and excision margin (Ex Margin) in 6 random high power microscopic fields (HPFs) are compared (*: $p < 0.01$, Student's *t*-test). The increased number of T cells, blood vessels and M2 macrophages in the margins of the excision indicates that patient's skin inflammation extends beyond the site of the cancer. Representative images are shown; ns: not significant; scale bar: 100μm.